International Journal of Recent Technology and Engineering (IJRTE)
ISSN: 2277-3878 (Online), Volume-8 Issue-2, July 2019

CFD Analysis of Magnetorheological Fluid Single Valve with an External Magnetic Field

Muhamad Husaini Abu Bakar, Mohamad-Syafiq Mohd-Kamal, Zahurin Samad

Abstract*: *Magnetorheological fluid (MRF) actuator emerged in the last decade as a potential system to replace electro-hydraulic servo system in precision applications. MRF actuator was control using a valve which is regulated with magnetic field. Because of valve performance relate with flow characteristic inside the valve, knowledge about the flow behaviour when magnetic field is applied was important. Currently analytical method was used to model the valve but limited into simple geometry. Reflect to the need of complex geometry of valve, CFD approached was used in this research work to model the fluid flow with presence of different magnetic strength magnitude as a result CFD model shows a good agreement with experiment with 3% error and the MRF velocity was reduce up to 85% when magnetic field applied. As conclusion, CFD model successfully develop and proven to be used as a tool in analysing the MRF flow.

Index Terms*: *Magnetorheological fluid valve, CFD, Electro-hydraulic, smart material.

I. INTRODUCTION

Accurate and precision positioning systems have emerged as a vital requirement in the industry [1]. Motorised actuators are popular choices in developing a positioning system over several decades. However, in a high load application, a motorised actuator is less efficient compared to a hydraulic actuator [1,2]. To this extent, an electro-hydraulic system has been introduced by many practitioners to answer the limitation of the motorised actuator system when a high load is needed [2,4,5]. The accuracy of the electro-hydraulic system is ensured by utilising a servo valve that is used to control the displacement of the cylinder. A conventional hydraulic control valve consists of a spool, inside which acts as a control mechanism. This spool is moved by a solenoid, and the speed of spool is determined by the current induced in the solenoid [6]. It is clear that proper control of the servo valve will help improve the accuracy and precision of a hydraulic positioning system.

The spool has introduced difficulty in controlling the valve due to friction with the valve body. Therefore, the magnetorheological fluid (MRF) valve was designed and has proven to control fluid flow.[7-11]. The MRF valve has successfully eliminated the use of a spool to control fluid flow by manipulating the MRF rheological properties using a magnetic field. The MRF is considered a smart material where its state might change from liquid to solid in milliseconds with the presence of magnetic field [12].The invention of the MRF valve potentially accelerates the development of an accurate positioning system. Even though the MRF valve was successfully designed to control the direction of the MRF, the valve is limited to simple geometry such as a straight channel. However, if the channel is complex, for example having a curvature, it becomes difficult for the MRF valve to regulate due to a lack of understanding fluid flow behaviour. Thus, the design process requires knowledge of fluid flow inside the valve while a magnetic field is applied.

Salloom and Samad (2012)[13] and Imaduddin et al. (2014)[8] developed an MRF valve that worked without a spool, but fluid behaviour in MRF valves have yet to be understood. Due to a lack in knowledge about MRF flow, the response of the valve is difficult to predict and the development of an optimal control system becomes slow. Even though Omidbeygi and Hashemabadi (2013)[14] solved the MRF fluid flow using an analytical solution, it is limited to simple geometry and strictly followed a 2D flow assumption due to limitation in analytical calculation, the aim of this work is modelling the MRF single valve using CFD to capture a complexity in geometry of the valve.

II. COMPUTATIONAL FLUID DYNAMIC ANALYSIS OF THE MRF VALVE

This section analyses the fluid flow behaviour inside the valve. CFD was used as a tool to simulate the fluid in critical areas such as the MRF channel and outlet plane. The simulation involved a steady analysis and was extended to transient in order to determine the mathematical representation of the plant model for the valve. In the steady analysis, the effect of the magnetic field on the Reynolds numbers was explored and the correlation function was developed. The simulation sequence started with pre-processing, followed by boundary condition setup, viscosity determination, and the solver setup.

III. MAGNETIC FIELD FUNCTION DEVELOPMENT VIA FINITE ELEMENT METHOD

The magnetic field generated by the current induced to the coil in the MRF valve channel was simulated using the finite element method.

Revised Manuscript Received on 30 July 2019.

***** Correspondence Author

Muhamad Husaini Abu Bakar*, Head of Research and Innovation, System Engineering and Energy Laboratory, Universiti Kuala Lumpur – Malaysian Spanish Institute, Kulim, Kedah, Malaysia.

Mohamad-Syafiq Mohd-Kamal, System Engineering and Energy Laboratory, Universiti Kuala Lumpur – Malaysian Spanish Institute, Kulim, Kedah, Malaysia.

Zahurin Samad, School of Mechanical Engineering, Universiti Sains Malaysia, Nibong Tebal, Pulau Pinang, Malaysia.

In this study, FEMM software was used as a tool to analyse the magnetic field response with current variation. A detailed explanation on the methodology to run the analysis was given by Salloom and Samad (2012) [13]. In short, the cross-section of the MRF valve was considered and drawn in the software, as shown in Fig 1.

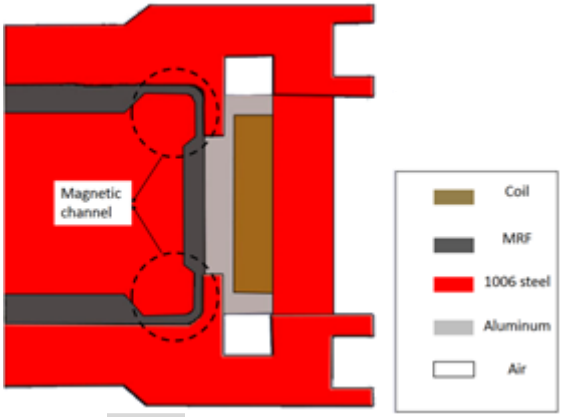

Fig. 1. MRF valve schematic

The valve channel was indicated as MRF and the casing named as 1006 steel. For the coil area, the copper wire with a diameter of 0.315 mm with 120 turns was set to approximate the real coil used in the valve. The material configuration is an important factor to minimise the flux leakage during operation. The 1006 steel was selected because its magnetic permeability is high enough to allow magnetic flux to flow narrowly in a curve channel with low reluctance. Aluminium with low permeability was used to prevent the flux from flowing to other areas. By narrowing the flux flow, the magnetic strength was higher at the focused area despite low current supply to the coil. The purpose of a narrow flux flow is to optimise the energy used in controlling the system. Theoretically, minimising the current helps reduce the heat increase in the coil due to losses that result from the internal resistance of the wire. Besides that, by concentrating the magnetic field on the narrow area, the magnetic loss was reduced. Hence, all the magnetic energy was used to solidify the fluid instead of being stored inside the magnetic circuit. The storage magnetic field in the circuit is commonly called a reminisce. This reminisce will introduce the magnitude of the magnetic field strength when no current is induced in the coil. Having a small magnitude of magnetic field in the channel potentially altered the nominal viscosity of the fluid. This phenomenon introduced disturbances to the valve, such as lagging time for viscosity change, which finally led to low transient response.

A two-dimensional cross-section drawing was then meshed with 65,000 elements, as shown in Fig. 2. The magnetic induction governing equation was finally solved using the finite element method. The magnetic contour was plotted, as shown in Fig. 3. Details of the flux flow magnitude and direction in the narrow curve channel was investigated.

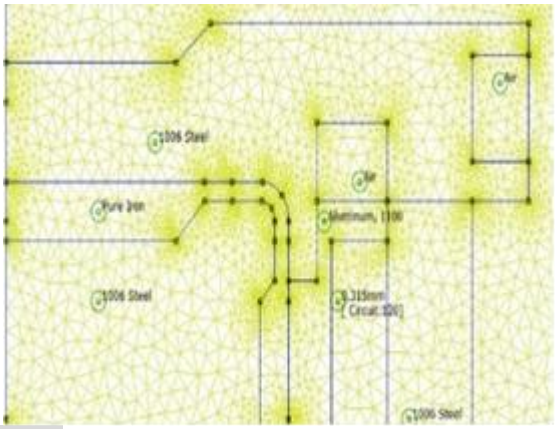

Fig. 2. Finite element modelling for MRF valve

The simulation was performed again with the value of the current varying from 0 to 2.4A in order to develop a mathematical correlation between the magnetic field and current. Fig. 3(b) presents the detailed flux line and the magnetic strength in the focused area. To reduce the error for CFD simulation, the direction of the flux was checked perpendicular to the fluid flow. Fig. 3(b) shows that the flux direction to the valve curve surface is normal. Besides that, the homogeneity of the magnetic strength in the channel valve is important. The contour plot shows that the magnetic strength is homogenous in this area, except at the curved area. By ensuring the homogeneity of the magnetic field in the channel, an important assumption can be made; the magnetic field in the focused area was approximated with the average value.

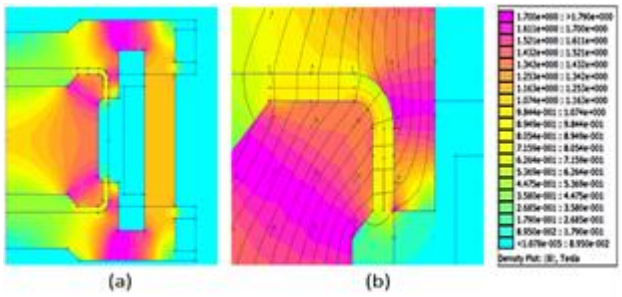

Fig. 3. Example of contour plot for magnetic field in the MRF valve: *(a)* Full valve *(b)* Magnetic corner area

A. Viscosity Model

The main difficulty in the modelling of MRF was due to its viscosity change dependent on the magnetic field. The viscosity of the fluid in the magnetic channel varied with changes in the magnetic field. Since the magnetic field was specifically applied to the selected area, the viscosity was only changed in the area indicated as the magnetic channel in Fig. 1. The viscosity behaviour needed to be modelled correctly in order to reduce the error in simulation. In this research, viscosity was related to the current induced by the coil. In the experiment, the current varied as an input, thereby requiring the determination of the correlation between current and viscosity. A few procedures were required to be observed in order to correlate the current to the viscosity, as shown in Fig. 4. From the reference current, the magnetic field was calculated using the correlations that were developed using the finite element method.

Generally, the shear flow behaviour of the MRF was described by the Bingham constitutive equation, as given in Eq. (1)[15].

$$\tau = \tau_0(\mathrm{H}) + \eta_\infty \overset{o}{\gamma} \quad (1)$$

Where τo is the field dependent yields stress dependent on magnetic field (H). η_∞ is the nominal viscosity or viscosity in the absence of magnetic field and $\dot{\gamma}$ is the shear strain rate of the fluid. In the CFD analysis, the parameter that needed to be set was viscosity. Eq. (1) transformed into an apparent viscosity (η_∞) given by Eq. (2):

$$\eta_\alpha\left(\overset{o}{\gamma}, \mathrm{H}\right) = \frac{\tau_0(\mathrm{H})}{\gamma} + \eta_\infty \quad (2)$$

A computational adoption was required to implement this model in the ANSYS software. Eq. (2) shows that the apparent viscosity became nominal viscosity in the absence of a magnetic field. Thus, the fluid had two viscous models, as shown in Eq. (3):

$$\eta_\alpha \begin{cases} \dfrac{\tau_0(\mathrm{H})}{\gamma} + \eta_\infty \overset{o}{\gamma} & \geq \overset{o}{\gamma_0} \\ \beta\eta_\infty \overset{o}{\gamma} & < \overset{o}{\gamma_0} \end{cases} \quad (3)$$

Where β is the non-dimensional parameter associated with the fluid stiffness in the pre-yield region. Bompos and Nikolakopoulos (2011)[16] set the value β as 100 because at this region, the fluid was in a viscoelastic form and the fluid moved only in small displacement. The bigger the value β, the better the consistency between the two viscosity models[13]. $\dot{\gamma}_0$ is the critical yield shear strain rate given by Eq. (4):

$$\overset{o}{\gamma_0} = \frac{\tau_0(\mathrm{H})}{(\beta - 1)\eta_\infty} \quad (4)$$

Eq. (4) was coded using the user-defined function (UDF) in the Fluent software. Eq. (3) and Eq. (4) clearly show that a field-dependent parameter should be determined in order to complete the simulation. Field-dependent shear stress ($\tau_0(\mathrm{H})$) was calculated with Eq. (5), as proposed by Nguyen *et al.* (2007)[17].

$$\tau_0(\mathrm{H}) = 52.962B^4 - 176.51B^3 + 158.79B^2 + 13.708B + 0.1442 \quad (5)$$

Where *B* is the magnetic flux density. This equation provided a correlation between fluid volume percentage, magnetic field, and shear stress. This approach was selected because it provided a better approximation for mixing MRF in laboratory, as proven by Grunwald and Olabi (2008)[7]. In this study, the volume percentage of iron filler in carrier fluid was constant at 0.32, while only the magnetic field varied. The shear stress predicted using Eq. (5) was used as the input to determine the viscosity shown in Eq. (4). Only then the viscosity in the magnetic channel was calculated and the Navier-Stokes equation solved by the solver.

IV. STEADY CFD ANALYSIS OF THE MRF VALVE

Fluid behaviour in an MRF valve gives a significant indicator of the final performance of the system. This section investigates the fluid flow behaviour of the MRF inside the valve channel. The characteristic of fluid in the presence of a magnetic field is explored to provide knowledge of pressure and volume flow rate during operation. The analysis started with the validation of the CFD code with experimental data. The study then developed a correlation between the parameters such as velocity profile, pressure drop, and volume flow rate of the valve.

A. Validation Study

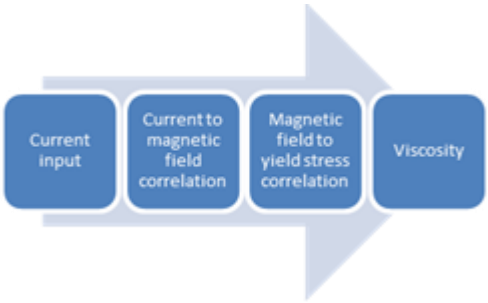

Fig. 4. Sequences of Steps in the Determination of Viscosity from Current Input to the Coil

It is a compulsory task to ensure that the CFD analysis follows real physical behaviours so that the data is reliable for use in analysing fluid behaviour. Fig. 5 shows a comparison of the CFD and the experimental data. The experimental data was taken at pressure 11 bar, but the current magnitude varied from 0 to 0.8A with an interval of 0.1A. The volume flow rate was recorded as a dependent variable for both the CFD and the experiment. The patterns that resulted from the CFD and the simulation are similar, proving that the CFD simulation successfully presented the real behaviour of the fluid. The average deviation was 2% with a minimum deviation of 1% and a maximum deviation of 4%.

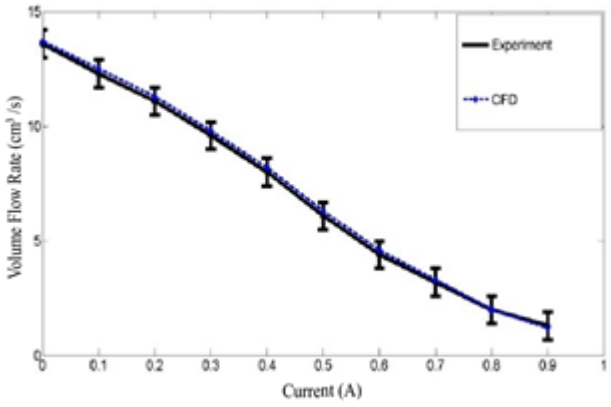

Fig. 5. CFD simulation and experimental results at pressure 11 bar

Although the deviation increased slightly (at current = 0.5A) when the current also increased, it is considered acceptable when the maximum deviation is under 5%. However, the deviation decreased when the current magnitude was in the range of 0.7 to 0.8A. Though the deviation occurred between the experiment and CFD data, the deviation is considered small compared to the value of the current range. This means that the quadratic function used is accurate from 0 to 2A. The second factor is the fluid nature where the Reynolds number reduced due to the increase in the current and the boundary layer of the flow increased.

To solve the problem of the boundary layer, a smaller mesh is required and dramatically increases the computational cost in terms of time. During the grid dependency study, the mesh was selected as an optimum element number to reduce the computational cost. This issue has a less significant effect on calculation. However, because the maximum error was less than 5%, the CFD model can then be used for further analysis and the result is reliable to present the fluid flow behaviour.

B. Effects of Magnetic Field on Volume Flow Rate

The most significant parameter in studying the performance of the MRF valve is the volume flow rate. The response of the volume flow rate with the current will affect the speed of linear motion of the cylindrical block. Fig. 6 shows the response of the volume flow rate for different current states. Linear fitting was used as a reference to indicate how the volume flow rate deviated from the linear line. This indicator is useful to measure the nonlinearity of the volume flow rate response to the current input. The volume flow rate does not correlate linearly when the current increased. Firstly, the correlation is inversely proportional, as shown by many other researchers such as Chooi and Oyadiji (2008)[18] and Sahin (2008)[19]. This phenomenon is because the increase in the current induced to the coil increases the magnetic field strength. According to Leicht et al. (2009)[20], increase in the magnetic field perpendicular to the fluid will increase the resistance to the MRF flow. Finally, the velocity of the fluid reduces the volume flow rate. Volume flow rate is proportionally related with the velocity of the fluid through the cross-section area, as mentioned in Gedik *et al.* (2012)[21] and Park *et al.* (2008)[22]. Thus, the volume flow rate will reduce when the current induced in the coil is increased. However, in Fig. 6 the reduction in the volume flow rate significantly deviated from the linear fitting, indicating that the relation is nonlinear. The nonlinearity issue was also highlighted by Omidbeygi and Hashemabadi (2012)[23], but the results are limited due to the difficulties in the setup. In this study, the CFD simulation was extended to many other points in order to fill the gap that was not supported by the experimental data. The R-square value, for when the data was fitted into cubic polynomial, was 0.99.

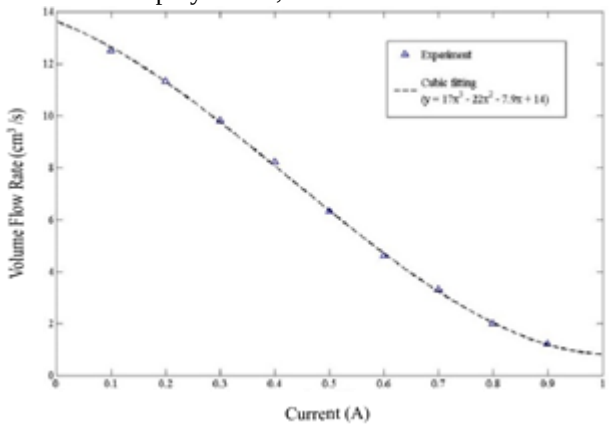

Fig. 6. Volume flow rate with changing in current at pressure drop 11 bar

C. Effects of Magnetic Field on Volume Flow Rate

The volume flow rate reduced with increasing magnetic field, as discussed previously. Since the volume flow rate was proportional to the velocity, it is important to understand the velocity behaviour when there are changes in the magnetic field. In this study, the area exposed to the magnetic field was in the corner channel, as shown in Fig. 7. Five lines at different positions were created to analyse the velocity profile

The fluid entered the corner channel at line a1 and flowed out at a5. The distance from wall to wall is also known as valve thickness, which in this case, equalled to 0.5 mm. The zero distance started from outer wall and the distance increased up to 0.5 mm when it reached the inner wall. For generality in discussion, the distance refers to the valve thickness and the profile of the velocity was plotted according to this thickness.

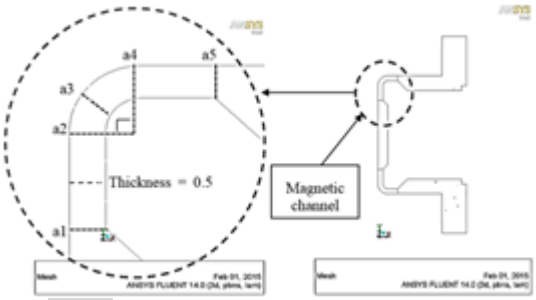

Fig. 7. Cross-Section of the MRF valve

Fig. 7 shows the CFD data of the MRF valve velocity profile at line a5 with respect to different current levels. In the graph, the normalised velocity represents the ratio between maximum velocity (U) and local velocity (U). The peak velocity of the flow when no current was applied to the coil is considered the maximum velocity. Maximum velocity is when no current induce is chosen because the viscosity of the fluid is considered Newtonian and there is no fluid resistance, except the wall friction acting on the system. Within this condition, the value of velocity becomes the highest for all study ranges.

Five current levels varied in this study, starting from zero to the maximum 0.8A, with a constant pressure at 11 bar. From the experiment, at current 0.8A, the fluid was still moving, but with low volume flow rate. The graph shows that the peak velocity was reduced by increasing the current. The fully developed profile pattern is similar to the analytical solution provided by Omidbeygi and Hashemabadi (2012).

An interesting parameter that can be extracted from the velocity profile plot in Fig. 8 is the percentage of reduction in peak velocity. To show how the peak velocity change in current variation, the graph peak velocity versus the current plot was used and shown in Fig. 9. Peak velocity reduced up to 20% when the current changed from zero to 0.2A. The peak velocity then reduced up to 30% when the current changed from 0.2 to 0.4A. The percentage of reduction in peak velocity value was 25% when the current varied from 0.4 to 0.6A. Finally, the velocity reduced 15% when the current was increased from 0.6 to 0.8A. From 0 to 0.8A, the velocity magnitude dropped up to 85% from the maximum velocity. However, the rate of change in the reduction of velocity was not constant and differed slightly at different current levels. At current levels from 0.6 to 0.8A, the percentage of reduction in peak velocity was low, as this was almost near saturation level.

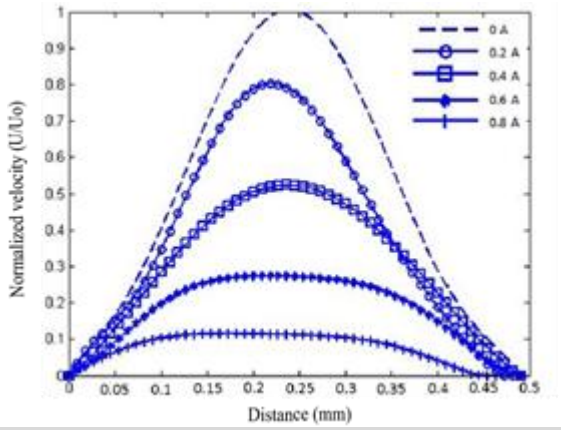

Fig. 8. Velocity profiles of simulated MRF along line a1

Beyond the level of 0.8A, the reduction rate reduced to zero and represented a constant peak velocity. In the case of high pressure, the fluid still moved even when the maximum current was applied to the coil. This is because the maximum magnetisation of the iron particle was exceeded, but the external force given was greater than the magnetic force needed to hold the particle together. This is why an asymptote line was created when the percentage of reduction was plotted for currents ranging 0.8A and above.

Details of the effect of the magnetic field on the fluid are shown in Fig. 10, where the comparison between no current and a current of 0.4A was made. Only two curves revealed the difference efficiently. With no current applied, the fluid behaved as Newtonian fluid, where the fully developed profile was almost in a parabolic form. This behaviour has been proven by an experiment [19], analytically [23], and numerically [21]. However, at a current of 0.4A, the velocity profile showed a significant difference from Newtonian fluid.

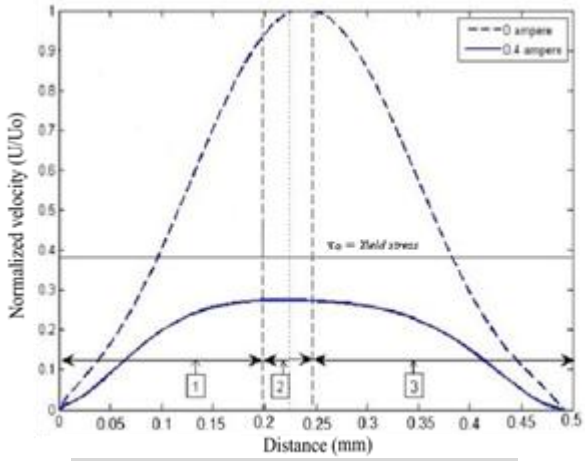

Fig. **10. Visco-Plastic behaviour of fluid**

The profile had a flat peak, where at a distance of 0.39 mm until 0.48 mm, the slope was zero, which means the velocity was constant. This behaviour is considered non-Newtonian fluid in the class of Bingham plastic fluid by Jha and Jain (2009)[24]. This type of flow is known as a plug flow by Chooi and Oyadiji (2008)[18] and Parlak and Engin (2012)[15]. Conventionally, this type of behaviour can be modelled with a Bingham plastic model. It can be characterised by the existence of threshold stress or in this case, yield stress. Yield stress must be exceeded to enable the flow of the fluid. In MRF, the yield stress varies by varying the magnetic field strength across the fluid domain. Parlak and Engin (2012)[15] named the flat peak as pre-yield, where the fluid nearly moves from static condition. Shivaram and Gangadharan (2007)[25] stated that the MRF yield stress increases with the increase in magnetic field, since the MRF obeys the Bingham plastic model. A profile pattern was compared at different positions, as shown in Fig. 11. For the next discussion, L1, L2, and L3 are used to indicate the same positions of a1, a2, and a3 in Fig. 9.

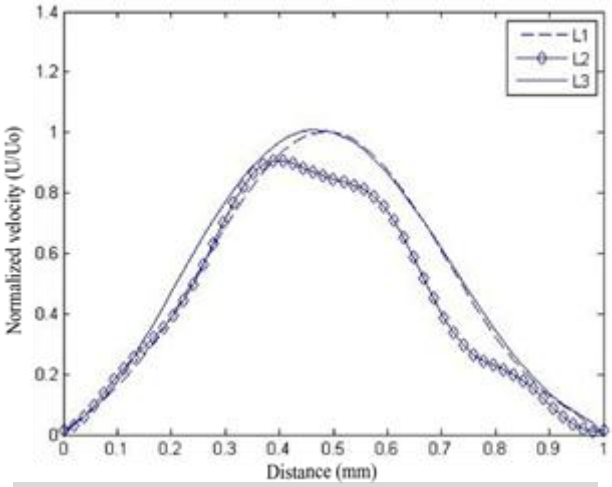

Fig. 11. Velocity profile of simulated MRF Flow for different positions with a current of 0.4A

The patterns for L1 and L3 were similar, as the position was at the interface area between the magnetic field and no magnetic field. At L2, there was a significant difference in the profile because its position was at the corner of the channel. At line L2, the fluid exposed to the magnetic field and the viscosity was relatively high compared to L1 and L3. With high viscosity, the resistance of the fluid to flow became higher. The profile at L2 consisted of two peaks and potentially created a secondary flow. The velocity magnitude of fluid at the outer wall was higher compared to the inner wall. This is because the flow at the outer wall has more momentum due to the geometry.

V. CONCLUSION

The CFD model for a steady and transient 3-dimensional flow of MRF inside a curvature channel was successfully developed using the CFD approach. The simulation result shows a small deviation with the experimental data at 3% and 4% error for steady and transient respectively. Furthermore, the finite element method was proven to be used as a tool to develop current and magnetic field correlation. Thus, the correlation finally reduced the complexity of modelling the viscosity of the MRF. The CFD model also gave significant conclusions as the following:

1) The volume flow rate decreased in cubic polynomial form when the magnetic field was increased;
2) The velocity profile pattern for the MRF flow in the channel was different when the magnetic magnitude was changed. By increasing the magnetic magnitude, the peak velocity was reduced and
3) The velocity magnitude reduced up to 85% when the current increased from 0 to 0.8 A.

NOMENCLATURE

τ : Shear stress (Pa)
τ_0 : Yield shear stress (Pa)
H : Magnetic field strength (A/m)
η_∞ : Nominal viscosity (Pa.s)
γ : Shear rate (s^{-1})
η_α : Apparent viscosity
Q : Flow rate (cm^{-3})
γ : Critical yield shear strain rate
B : Magnetic flux density (Tesla)
U : Velocity of MR fluid (cm/sec)
L : Length (mm)

ACKNOWLEDGMENT

It is optional. The preferred spelling of the word "acknowledgment" in American English is without an "e" after the "g." Use the singular heading even if you have many acknowledgments. Avoid expressions such as "One of us (S.B.A.) would like to thank ... ." Instead, write "F. A. Author thanks " *Sponsor and financial support acknowledgments are placed in the unnumbered footnote on the first page*.

REFERENCES

1. Wonohadidjojo, D., Kothapalli, G., & Hassan, M. (2013). Position Control of Electro-hydraulic Actuator System Using Fuzzy Logic Controller Optimized by Particle Swarm Optimization. International Journal of Automation and Computing, 10(3), 181–193. http://doi.org/10.1007/s11633-013-0711-3
2. Guo, Q., Yu, T., & Jiang, D. (2015). Robust H∞ positional control of 2-DOF robotic arm driven by electro-hydraulic servo system. ISA Transactions https://doi.org/10.1016/j.isatra.2015.09.014
3. A. B. M. Husaini & Z. Samad (2017). Vision-Based Positioning System for Magnetorheological Fluid Actuator Using NNARX. Advance Science Letters, 23, 4424-4428
4. https://doi.org/10.1166/asl.2017.8915
5. Le-Hanh, D., Ahn, K. K., Kha, N. B., & Jo, W. K. (2009). Trajectory control of electro-hydraulic excavator using fuzzy self tuning algorithm with neural network. Journal of Mechanical Science and Technology, 23 (1), 149-160.
6. https://doi.org/10.1007/s12206-008-0817-7
7. Lin, F. (2011). The Design and Simulation of Electro-Hydraulic Velocity Control System. In D. Li, Y. Liu, & Y. Chen (Eds.), Computer and Computing Technologies in Agriculture IV SE - 68 (Vol. 347,pp. 568-574). Springer Berlin Heidelberg. http://doi.org/10.1007/978-3-642-18369-0_68
8. Kang, Y., Chen, Y.-W., Chang, Y.-P., & Chu, M.-H. (2008). The Direct Neural Control Applied to the Position Control in Hydraulic Servo System. In F. Sun, J. Zhang, Y. Tan, J. Cao, & W. Yu (Eds.), Advances in Neural Networks - ISNN 2008 SE- 21 (Vol. 5264, pp. 180–189). Springer Berlin Heidelberg. http://doi.org/10.1007/978-3-540-87734-9_21
9. Grunwald, A., & Olabi, A. G. (2008). Design of magneto-rheological (MR) valve. Sensor and actuators A: Physical, 148(1), 211-223. http://doi.org/10.1016/j.sna.2008.07.028
10. Imaduddin, F., Mazlan, S. A., Rahman, M. A., Zamzuri, H., U., & Ichwan, B. (2014). A high performance magnetorheological valve with a meandering flow path. Smart Materials and Structures, 23(6), 065017. http://doi:10.1088/0964-1726/23/6/065017
11. Moon, S.-J., Huh, Y.-C., Jung, H.-J., Jang, D.-D., & Lee, H.-J. (2011). Sub-optimal design procedure of valve-mode magnetorheological fluid dampers for structural control. KSCE Journal of Civil Engineering, 15(5), 867–873. http://doi.org/10.1007/s12205-011-1178-9
12. Hadadian, A., Sedaghati, R., & Esmailzade (2014). Design optimization of magnetorheological fluid valves using response surface method. Journal of Intelligent Material Systems and Structures, 25(11),1352–1371. https://doi.org/10.1177/1045389X13504478
13. Husaini, A., Izzat, G., Zahurin, S., & Rusli, O. (2013). Development of Machine Vision Positioning System of Magnetorheological Fluid (MRF) Actuator. Applied Mechanics and Materials, 470, 625-629. doi:10.4028/www.scientific.net/amm.470.625
14. Ekwebelam, C., & See, H. (2009). Microstructural investigations of the yielding behaviour of bidisperse magnetorheological fluids. Rheologica Acta, 48(1), 19–32. http://doi.org/10.1007/s00397-008-0297-9
15. Salloom, M., & Samad, Z. (2012). Magneto-rheological directional control valve. The International Journal of Advanced Manufacturing Technology, 58(1-4), 279– 292. http://doi.org/10.1007/s00170-011-3377-4
16. Omidbeygi, F., & Hashemabadi, S. H. (2013). Exact solution and CFD simulation of magnetorheological fluid purely tangential flow within an eccentric annulus. International Journal of Mechanical Sciences, 75, 26–33. http://doi.org/10.1016/j.ijmecsci.2013.04.009
17. Parlak, Z., & Engin, T. (2012). Time-dependent CFD and quasi-static analysis of magnetorheological fluid dampers with experimental validation. International Journal of Mechanical Sciences, 64(1), 22–31. http://doi.org/10.1016/j.ijmecsci.2012.08.006
18. Bompos, D. A., & Nikolakopoulos, P. G. (2011). CFD simulation of magnetorheological fluid journal bearings. Simulation Modelling Practice and Theory, 19(4). https://doi.org/10.1016/j.simpat.2011.01.001
19. Nguyen, Q., Han, Y., Choi, S., & Wereley, N. M. (2007). Geometry optimization of MR valves constrained in a specific volume using the finite element method. Smart Materials and Structures,16(6), 2242-2252. doi:10.1088/0964-1726/16/6/027
20. Chooi, W. W., & Oyadiji, S. O. (2008). Design, modelling and testing of magnetorheological (MR) dampers using analytical flow solutions. Computers & Structures, 86(3-5), 473–482. http://doi.org/10.1016/j.compstruc.2007.02.002.
21. Sahin, H. (2008). Theoretical and experimental studies of magnetorheological (MR) fluids and MR greases/gels: From rheology to system application. ProQuest Dissertations and Theses. University of Nevada, Reno, Ann Arbor. Retrieved from http://search.proquest.com/docview/276094176?accountid=14645
22. Leicht, Z., Urreta, H., Sanchez, A., Agirre, A., Kuzhir, P., & Magnac, G. (2009). Theoretical and experimental analysis of MR valve. Journal of Physics: Conference Series,149, 012070. doi:10.1088/1742-6596/149/1/012070
23. Gedik, E., Kurt, H., Recebli, Z., & Balan, C. (2012). Two-dimensional CFD simulation of magnetorheological fluid between two fixed parallel plates applied external magnetic field. Computers & Fluids, 63, 128–134. http://doi.org/10.1016/j.compfluid.2012.04.011
24. Park, E. J., da Luz, L. F., & Suleman, A. (2008). Multidisciplinary design optimization of an automotive magnetorheological brake design. Computers & Structures, 86(3-5), 207–216. http://doi.org/10.1016/j.compstruc.2007.01.035
25. Omidbeygi, F., & Hashemabadi, S. H. (2012). Experimental study and CFD simulation of rotational eccentric cylinder in a magnetorheological fluid. Journal of Magnetism and Magnetic Materials, 324(13), 2062–2069. http://doi.org/10.1016/j.jmmm.2012.02.016
26. Jha, S., & Jain, V. K. (2009). Rheological characterization of magnetorheological polishing fluid for MRAFF. The International Journal of Advanced Manufacturing Technology, 42(7-8), 656–668. http://doi.org/10.1007/s00170-008-1637-8

AUTHORS PROFILE

First Author Muhamad Husaini Abu Bakar is Director for System engineering and Energy Laboratory and Head of Research and Innovation Section at the Universiti Kuala Lumpur – Malaysian Spanish Institute,Malaysia. Having obtained a Bachelor Degree in Manufacturing Engineering with Management at the Universiti Sains Malaysia (2007), Malaysia, he spent the time from 2007–2012 at the Underwater Robotic Research Group, Universiti Sains Malaysia as a research engineer and awarded Master of Science in advance manufacturing from Universiti Sains Malaysia in 2011. Since 2012 he work as lecturer at Universiti Kuala Lumpur – Malaysian Spanish Institute and obtain his Doctor of Philosophy in Advanced Manufacturing from Universiti Sains Malaysia in 2017. His research interests are related to smart manufacturing, energy, and atomistic modelling.

Second Author Mohamad-Syafiq Mohd-Kamal is Master student of System Engineering and Energy Laboratory at the Universiti Kuala Lumpur – Malaysian Spanish Institute,Malaysia. Background of study in Bachelor Engineering Technology (Hons.) Mechatronics at Universiti Kuala Lumpur – Malaysian Spanish Institute. His research interest are related to Quantum Modelling, Energy (Metal-air Batteries), corrosion inhibitor, automation and control system. His research activities focusing on corrosion inhibitor at aluminium-air battery.

Third Author Zahurin Samad is Associate Professor School of Mechanical Engineering at the Universiti Sains Malaysia, Malaysia. Having obtained a Bachelor of Science at Northrop. Awarded Master of Science at Swansea and obtain his Doctor of Philosophy at Leeds. His specialize in Manufacturing Automation, Robotics, Control System, Machine Visions, Machine Equipment CNC, Neural Networks, Artificial Intelligent PLC, Computer Aided Manufacturing Solar Detection System. His Research area are Automation, Robotics, Machine Vision, Control System, Neural Network.